Positioning based on OFDM signals through phase measurements

Dun, Han; Tiberius, Christiaan; Janssen, Gerard

Publication date
2018

Document Version
Accepted author manuscript

Published in
Conference proceedings of the NaviTec 2018, the 2018 9th ESA Workshop on Satellite Navigation Technologies and European Workshop on GNSS Signals and Signal Processing (NAVITEC)

Positioning based on OFDM Signals through Phase Measurements

5-7 December 2018
ESA/ESTEC, Noordwijk, The Netherlands

Han Dun[(1)], Christian C. J. M. Tiberius[(1)], Gerard J. M. Janssen[(2)]

[(1)]Geoscience and Remote Sensing, Delft University of Technology
Delft, The Netherlands
Email:{h.dun, c.c.j.m.tiberius}@tudelft.nl

[(2)]Circuits and Systems, Delft University of Technology
Delft, The Netherlands
Email: g.j.m.janssen@tudelft.nl

ABSTRACT
High accuracy terrestrial radio positioning systems, as a complement to a global navigation satellite system (GNSS), are attracting significant attention from academia and industry. This article investigates the feasibility of positioning based on carrier phase measurements of orthogonal frequency division multiplexing (OFDM) signals. Generally, the carrier phase cannot be obtained from a baseband central carrier (i.e., direct current (DC) subcarrier) of OFDM signals, so we derived the carrier phase by calculating the average phase from two symmetrically located pilot sub-carriers. The sampling clock error and the timing synchronization error, which often occur in practice, can be cancelled by measuring the phase difference between two symmetrically located sub-carriers. The presented approach is simulated for a positioning system based on IEEE 802.11p Wireless LAN. Due to the presence of an initial carrier phase offset, the integer carrier phase ambiguity can, as expected, not be properly resolved. Although we can only obtain a 'float' solution from the observation model, the position accuracy can still achieve decimetre level.

INTRODUCTION

Today our society heavily relies on the global navigation satellite system (GNSS) for positioning and navigation. It has an excellent proven track record, and a very high economic value, but it also has a number of limitations. Its positioning performance is especially sensitive to atmospheric distortion. Due to a relative narrow signal bandwidth, the receiver cannot distinguish the direct light-of-sight (LoS) path from the reflection paths very well if the arrival times of these signals are close together. This leads to limited positioning accuracy. Compared to GPS signals, some existing wireless communication signals have a wider signal bandwidth and larger signal power. Although these signals are not designed for positioning, they still contain certain features that can be exploited for positioning, for example, time delay measurements and carrier phase measurements. Thus, these signals can be referred to as signals-of-opportunity (SOP) for positioning and navigation.

Orthogonal frequency division multiplexing (OFDM) signals can be found in various telecommunication systems, such as Wireless LAN (WLAN), terrestrial digital video broadcast (DVB-T), long-term evolution (LTE) and other wireless communication system. Recently, a number of studies on positioning based on OFDM signals have been conducted. They can be divided into two categories: based on received signal strength (RSS) and those based on time delay estimation.

RSS is a mandatory feature in standard compliant OFDM-based devices. Thus it is easy to derive and collect measurements of RSS. Using fingerprinting or geometric approaches which are based on RSS propagation models, the position of the receiver can be derived. However, despite all effort and optimization, RSS-based positioning can only achieve a 1-3 meter accuracy on average in LoS propagation scenarios [1], [2], [3].

Time delay estimation-based positioning requires a very high accuracy time-of-arrival (ToA) estimation (e.g., sub-3 ns for sub-meter ranging). Makki *et. al.* [4] [5] proposed a ToA estimation algorithm based on OFDM signals, which consists of two steps, cross-correlation based coarse estimation, and channel estimation based fine adjustment. This method can achieve a sub-meter level accuracy (0.42m) in a low multipath environment. In addition, some super-resolution methods, which separate the signal subspace from the noise subspace using eigenvalue decomposition of the correlation matrix, also have been investigated for ToA estimation. Super-resolution approaches such as MUSIC and ESPRIT [6] have been shown to achieve a meter-level accuracy in a multipath scenario. Since the signal bandwidth is one of the key factors affecting the accuracy of ToA estimation in a multipath propagation environment [7], Vasisht *et. al.* [8] utilized frequency hopping among different frequency bands to emulate a wideband multi-GHz radio, and presented a decimetre level positioning system using a single Wi-Fi access point. By 'stitching' multiple signal bands together, the multipath effect can be mitigated.

Alternatively, considering a signal with a fixed and possibly narrow bandwidth, this wireless signal should be always modulated on a carrier within a relatively high frequency (GHz-level). For a given phase measurement accuracy, a short carrier wavelength gives a better distance accuracy, though the phase ambiguities need to be resolved. Thus, tracking the carrier phase of OFDM signals can potentially lead to a more accurate ranging and positioning performance. Carrier phase measurements have been used in GPS for accurate positioning [9], however, research on positioning based on OFDM signals through phase measurements is still limited. So far, only Yang *et. al.* [10] investigated the feasibility of tracking the carrier phase of OFDM based DVB-T signals, in which the DC component is retained as a

pilot sub-carrier and provides a possibility to track the carrier phase directly. But in that DVB-T based system, the carrier phase measurement can only be obtained after compensating the sampling clock offset (SCO) and the carrier frequency offset (CFO). Since the CFO is partially introduced by the Doppler effect due to mobility of the receiver, the approach applied in [10] can only be applied to a static receiver. Though SCOs and CFOs were estimated and compensated to their best, the performance of the carrier phase tracking is limited by the clock mismatch between the transmitter and receiver.

In fact, the DC subcarrier of most baseband OFDM signals is generally allocated as a null sub-carrier so as to avoid the effect of a DC bias at the receiver.

In this research, we aim to investigate the feasibility of positioning based on OFDM signals through non-DC pilot sub-carriers, which can be used for carrier phase tracking. Since the carrier phase cannot directly be measured because the DC component is a null sub-carrier, we combined the measured phases from two symmetrically located pilot sub-carriers to interpolate the phase of the carrier frequency. Moreover, the sampling clock error and the timing synchronization error that depend on the subcarrier index can be cancelled through this combination. In addition, we simulate an IEEE 802.11p-like based positioning system to demonstrate the effectiveness of the proposed method.

OFDM SIGNAL MODEL

An OFDM symbol is generated by modulating N complex data points using the inverse discrete Fourier transform (IDFT) on N sub-carriers [11]. In order to combat inter-symbol interference (ISI) caused by a multipath channel, a guard interval (i.e., cyclic prefix-CP) with a repetition of the last N_g samples is added to every OFDM symbol. Thus, there are N_g+N samples in each OFDM symbol. Then, the n-th sample of the l-th OFDM symbol ($l \geq 0$) in baseband can be given as

$$s[l;n] = \frac{1}{N} \sum_{k=-N/2+1}^{N/2} c_{k,l} e^{j\frac{2\pi(l(N+N_g)+N_g+n)k}{N}}, \quad n = \begin{cases} -N_g,...,-1 \text{ (CP)} \\ 0,...,N-1 \text{ (Data)} \end{cases}$$

Where k denotes the subcarrier index from $-N/2+1$ to $N/2$, and $c_{k,l}$ denotes the complex data of the l-th symbol modulated on the k-th sub-carrier.

After passing through a digital-to-analog converter (DAC), the baseband OFDM signal $s(t)$ is modulated on a carrier with frequency f_C. Hence, the passband OFDM signal $s_p(t)$ can be expressed as

$$s_p(t) = \Re\left\{ s(t) e^{j2\pi f_c t} \right\}, \quad t = \left(l(N+N_g) + N_g + n \right) T_s$$

where $\Re$ denotes the real part of a complex value, T_s denotes the sampling interval. At the receiver, the passband signal through a channel should be down-converted to baseband with the same carrier frequency f_c. Thus, the received baseband signal is given as

$$r_b(t) = 2\mathcal{F}_L \left\{ (s_p(t) * h(t)) \cos(2\pi f_c t + \theta) \right\} + j2\mathcal{F}_L \left\{ -(s_p(t) * h(t)) \sin(2\pi f_c t + \theta) \right\}, \quad (1)$$

where $\mathcal{F}_L$ denotes a low pass filter, $(*)$ denotes the convolution operator, j denotes an imaginary unit, $h(t)$ denotes the channel impulse response, and θ denotes the initial carrier phase offset of the carrier frequency generated at the receiver compared with that generated at the transmitter.

In order to demodulate the received OFDM signal properly, timing synchronization should be conducted to find the start point of an FFT window. The CFO and the SCO should also be estimated and compensated as precisely as possible. However, for the purpose of positioning, we are only interested in the carrier phase. By means of a linear combination of sub-carriers phase measurements, some offset terms can be cancelled. Though the combination is meaningless in terms of the data demodulation, it provides an opportunity to track the carrier phase measurements. The impact of these offsets, specifically for the carrier phase, are described in the following subsections.

Carrier frequency offset (Doppler frequency offset)

The carrier frequency offset is mainly caused by the mismatch of the locally generated RF carrier frequency at the receiver and the Doppler effect. However, from the perspective of carrier phase-based positioning, we are only interested in the change of the carrier phase (or carrier frequency offset) due to the Doppler effect, because the geometric information of the receiver can be retrieved by tracking the carrier phase. Hence, we assume that the carrier frequency offset due to the mismatched locally generated central carrier frequency can be calibrated or compensated during the initial stage to a certain level and can be ignored, thus only the carrier frequency offset due to the Doppler effect remains.

Consider an OFDM rover receiver in a kinematic ranging scenario as shown in Fig. 1, in which the moving receiver acquires signals continuously, and the LoS propagation channel can be modeled as

$$h(t) = \alpha\delta(t - \tau_1(t)), \quad \tau_1(t) = \tau_1' - \int_0^t \frac{v\cos(\theta(v))}{c} \mathrm{d}v, \quad (2)$$

where α denotes the relative attenuation of the signal amplitude. In a relative small scale positioning scenario, α is assumed as a constant value. In addition, $\delta(\cdot)$ denotes the Dirac function, τ_1' denotes the initial propagation delay of the LoS path at t=0 in terms of Tx3 (e.g., (0,0) in this example), $\theta(t)$ denotes the time-dependent angle-of-arrival of the LoS signal, v denotes the velocity of the receiver, c denotes the speed of light, and $[0, t]$ denotes the observation period.

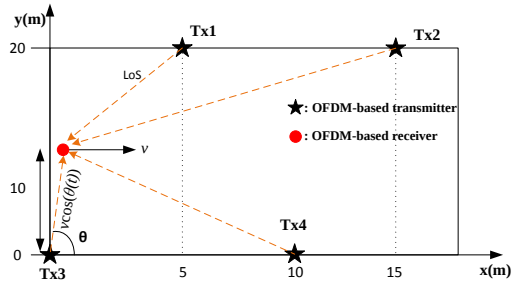

Fig. 1 A 2-D roadway positioning scenario: four transmitters with fixed and known locations and one rover receiver with a constant velocity, indicated by the black arrow.

Thus, the instantaneous Doppler frequency shift of the *i*-th sub-carrier can be described by

$$f_{D,i}(t) = (f_c + f_i)\frac{v\cos(\theta(t))}{c}. \tag{3}$$

Furthermore, we assume that the channel (also including the Doppler shift) is quasi-stationary within one OFDM symbol, in other words, the channel does not change within one OFDM symbol (e.g., 8 μs with a 10MHz bandwidth), but can vary from symbol to symbol. Thus, equation (3) can be rewritten as a function of the OFDM symbol index *l*

$$f_{D,i,l} = (f_c + f_i)\frac{v\cos(\theta_l)}{c}, \tag{4}$$

where θ_l denotes the angle-of-arrival of the received *l*-th symbol.

Sampling Clock Offset

The mismatch of the sampling clock frequency between a receiver and a transmitter, which we also refer to as the sampling clock offset (SCO), will lead to a linear phase drift over sub-carriers. It is common to put the sampling clock offset at the receiver side, thus the sampling clock error at the transmitter is zero. The received baseband OFDM signal in (1) can be rewritten as

$$r_b[l;n;\eta] = r_b(t), \quad t = \left(l(N+N_g)+N_g+n\right)(1+\eta)T_s, \tag{5}$$

where T_s denote the sampling interval at the transmitter, η denotes the sampling clock offset at the receiver, thus the sampling interval at the receiver can be given as $(1+\eta)T_s$.

Due to the Doppler frequency offset and the propagation channel, the received signal can be expressed as

$$r_b[l;n;\eta] = \frac{\alpha}{N}\sum_{i=-N/2+1}^{N/2} c_{i,l}\exp\left(j\left(\frac{2\pi i\left(l(N+N_g)+N_g\right)\eta}{N}+\frac{2\pi in(1+\eta)}{N}\right)\right)\exp\left(-j\left(2\pi\left(\psi_{D,i,l}+f_{D,i,l}n(1+\eta)T_s\right)+\theta\right)\right), \tag{6}$$

where $\psi_{D,i,l}$ denotes the integrated Doppler carrier phase of the CP on the *i*-th sub-carrier of the *l*-th symbol, and is given as

$$\psi_{D,i,l} = (f_c + f_i)\tau_1' + f_{D,i,l}N_g(1+\eta)T_s + \phi_{D,i,l-1}';\ \ f_i = i/(NT_s). \tag{7}$$

And $\phi_{D,i,l-1}'$ denotes the change of the Doppler phase included the impact of the SCO on the *i*-th sub-carrier from the previous (*l*-1) OFDM symbols, which can be given as

$$\phi_{D,i,l-1}' = \sum_{p=0}^{l-1}(N+N_g)f_{D,i,p}(1+\eta)T_s, \quad l \geq 1.$$

Timing Synchronization Error

Due to the sampling clock offset, the OFDM system cannot always achieve a perfect timing synchronization. However, we can still assume that the FFT window can always start in the CP. Thus, there is no ISI in an OFDM system. Considering the timing synchronization error $\Delta \in [0, N_g)T_s$, the only consequence of this timing offset error in the frequency domain is a linear proportional phase rotation on every sub-carrier. Therefore, the received data on the *k*-th subcarrier of the *l*-th symbol can be given as

$$
\begin{aligned}
R_{k,l} &= \mathcal{F}\{r_b[l;n;\eta]\}\exp\left(-j\frac{2\pi k\Delta}{N}\right)=\left(\sum_{n=0}^{N-1} r_b[l;n;\eta]\exp\left(-j\frac{2\pi kn}{N}\right)\right)\exp\left(-j\frac{2\pi k\Delta}{N}\right) \\
&= \frac{\alpha}{N}\sum_{i=-N/2+1}^{N/2}\left(c_{i,l}\exp\left(j\frac{2\pi iN_l\eta}{N}\right)\exp\left(-j\left(2\pi\psi_{D,i,l}+\theta\right)\right)\varpi\right)\exp\left(-j\frac{2\pi k\Delta}{N}\right); \\
\varpi &= \sum_n\left(\exp\left(j\frac{2\pi ni(1+\eta)}{N}\right)\exp\left(-j2\pi f_{D,i,l}n(1+\eta)T_s\right)\exp\left(-j\frac{2\pi nk}{N}\right)\right),\ N_l = l(N+N_g)+N_g,
\end{aligned}
\tag{8}
$$

where $\mathcal{F}$ denotes the Fourier transform.

According to (8), the Doppler shift will result in inter-carrier interference (ICI). Assume that ICI mainly impacts on neighboring sub-carriers (i.e., the (*k*-1)-th and (*k*+1) sub-carriers), the received data on the *k*-th sub-carrier, which consists of the desired signal term and the interference terms, can be further rewritten as

$$
R_{k,l} = \frac{\alpha}{N}\exp\left(-j\frac{2\pi k\Delta}{N}\right)\left(c_{k,l}\exp\left(j\left(\frac{2\pi kN_l\eta}{N}-2\pi\psi_{D,k,l}-\theta\right)\right)\sum_{n=0}^{N-1}\exp\left(j\frac{2\pi n\left(\eta k-f_{D,k,l}(1+\eta)NT_s\right)}{N}\right)+\text{ICI}\right). \tag{9}
$$

POSITIONING MODEL BASED ON PHASE MEASUREMENTS

From the perspective of data communication, the CFO and the SCO must be accurately estimated and compensated before demodulating the data. However, the CFO due to Doppler contains the geometric information. So instead of compensating for the CFO, we can track the Doppler frequency offset which can then be used to determine the position of the receiver. In an OFDM system, tracking the carrier frequency offset can generally be achieved by tracking the sub-carrier phase based on the channel estimation.

Moreover, if the value of the term $\left(\eta k-f_{D,k,l}(1+\eta)NT_s\right)$ in (9) is relative small, we can have the following approximation

$$
\sum_n\exp\left(j\frac{2\pi n\left(\eta k-f_{D,k,l}(1+\eta)NT_s\right)}{N}\right)\approx N\exp\left(j\pi\left(\eta k-f_{D,k,l}(1+\eta)NT_s\right)\right). \tag{10}
$$

And given a relative narrow signal bandwidth, the inter-carrier interference (ICI) in (9) is still negligible as long as the subcarrier spacing is considerably larger than the carrier frequency offset. In addition, if $\eta \ll 1$, the integrated Doppler carrier phase $\Psi_{D,k,l}'$ on the *k*-th subcarrier of the *l*-th symbol can further be simplified as

$$
\Psi_{D,k,l}' = (f_c+f_k)\tau_1' + f_{D,k,l}(N_g+N/2)(1+\eta)T_s+\phi_{D,k,l-1}' \approx (f_c+f_k)\tau_1' + f_{D,k,l}(N_g+N/2)T_s+\phi_{D,k,l-1}'. \tag{11}
$$

Thus, equation (9) can be further rewritten as

$$
R_{k,l}\approx\alpha c_{k,l}\exp\left(-j\frac{2\pi k\Delta}{N}\right)\exp\left(j\left(2\pi\left(\frac{k\left(l(N+N_g)+N_g+N/2\right)\eta}{N}-\Psi_{D,k,l}'\right)-\theta\right)\right).
$$

Considering the sampling clock offset η and timing synchronization error Δ, the phase obtained from the channel estimation can be given as

$$
\Phi_k(l)=\arg\left(\frac{R_{k,l}}{c_{k,l}}\right)\approx 2\pi\left(\frac{k\left(l(N+N_g)+N_g+N/2\right)\eta}{N}-\Psi_{D,k,l}'-\frac{k\Delta}{N}\right)-\theta. \tag{12}
$$

In addition, the phase obtained from (12) is always in the range of $[-\pi,\ \pi]$. In order to continuously track the carrier phase and keep the unknown phase ambiguity constant, phase measurements should be unwrapped. However, the timing synchronization error Δ may vary from frame to frame, which can potentially lead to a cycle-slip or even a failure of phase unwrapping. Alternatively, we can simply use two symmetrically located pilot sub-carriers to cancel it instead and construct the carrier phase. Hence, the average phase from two subcarriers can be derived as

$$
\Phi_{-k,k}(l)=\frac{1}{2}\left(\Phi_k(l)+\Phi_{-k}(l)\right)\approx -2\pi\left(f_c\tau_1'+f_{D,c,l}(N_g+N/2)T_s+\phi_{D,c,l-1}'\right)-\theta, \tag{13}
$$

where $f_{D,c,l}$ denotes the carrier frequency offset due to Doppler from the RF carrier f_c in the *l*-th OFDM symbol. Like (4), $f_{D,c,l}$ is defined as

$$
f_{D,c,l}=f_c\frac{v\cos(\theta_l)}{c}.
$$

Thus, the Doppler phase change on the carrier over the previous *l*-1 OFDM symbols can be expressed as

$$
\phi_{D,c,l-1}'=\sum_{p=0}^{l-1}(N+N_g)f_{D,c,p}(1+\eta)T_s.
$$

In addition, in order to keep the integer phase ambiguity constant, the phase measurement should be unwrapped. The unwrapped phase measurement in the l_1-th OFDM symbol, which is referred to as epoch t_1, can be derived from the channel estimation as

$$\begin{aligned}\underline{\Phi}_{-k,k}(t_1) &\approx -2\pi\left(f_c\tau_1' + f_{D,c,l_1}(N_g + N/2)T_s + \phi_{D,c,l_1-1}'\right) - \theta + \underline{e}(t_1) \\ &= -2\pi f_c \frac{\sqrt{(x-a(t_1))^2 + (y-b(t_1))^2}}{c} + 2\pi M - \theta + \underline{e}(t_1),\end{aligned} \tag{14}$$

where the random variables are denoted with underscore, x and y denote the known coordinates of the transmitter, $a(\cdot)$ and $b(\cdot)$ denote the unknown coordinates of the receiver in a 2D positioning scenario, M denotes the integer phase ambiguity, and θ denotes the initial carrier phase offset between the transmitter and receiver, e denotes the noise component in terms of the first transmitter .

In fact, the initial carrier phase offset θ in (14) cannot be separated from the initial integer phase ambiguity M. Without using the double-difference technique as in GNSS or calibrating this initial phase offset, we are unable to retrieve an integer phase ambiguity. Thus, we only estimate the phase ambiguity M_f as a float number instead, which remains constant over the observation period as long as the carrier phase can continuously be tracked and successfully unwrapped.

For clarity, we let the geometric distance between the i-th transmitter and the receiver at the time epoch t_1 as

$$r_i(t_1) = \sqrt{(x_i - a(t_1))^2 + (y_i - b(t_1))^2}, \tag{15}$$

where x_i and y_i denote the known coordinates of the i-th transmitters. Based on the aforementioned phase measurements at two epochs t_1 and t_2 on the signals of four transmitters, the estimation problem becomes solving the following sets of equations

$$\begin{aligned}
\underline{\Phi}^1_{-k,k}(t_1) &= -2\pi f_c r_1(t_1)/c + 2\pi M_{f,1} + \underline{e}_1(t_1) \\
\underline{\Phi}^2_{-k,k}(t_1) &= -2\pi f_c r_2(t_1)/c + 2\pi M_{f,2} + \underline{e}_2(t_1) \\
\underline{\Phi}^3_{-k,k}(t_1) &= -2\pi f_c r_3(t_1)/c + 2\pi M_{f,3} + \underline{e}_3(t_1) \\
\underline{\Phi}^4_{-k,k}(t_1) &= -2\pi f_c r_4(t_1)/c + 2\pi M_{f,4} + \underline{e}_4(t_1) \\
\underline{\Phi}^1_{-k,k}(t_2) &= -2\pi f_c r_1(t_2)/c + 2\pi M_{f,1} + \underline{e}_1(t_2) \\
\underline{\Phi}^2_{-k,k}(t_2) &= -2\pi f_c r_2(t_2)/c + 2\pi M_{f,2} + \underline{e}_2(t_2) \\
\underline{\Phi}^3_{-k,k}(t_2) &= -2\pi f_c r_3(t_2)/c + 2\pi M_{f,3} + \underline{e}_3(t_2) \\
\underline{\Phi}^4_{-k,k}(t_2) &= -2\pi f_c r_4(t_2)/c + 2\pi M_{f,4} + \underline{e}_4(t_2),
\end{aligned} \tag{16}$$

where the superscript of $\Phi^{(\cdot)}_{-k,k}$ denotes the index of the transmitter, f_c denotes the carrier frequency, $M_{(f,.)}$ denotes the unknown float phase ambiguity.

Equation (16) presents nonlinear least-squares estimation problem, which can be solved, for instance, by the Gauss-Newton method [12]. Applying the Taylor series expansion to (15) and ignoring the higher order terms, equation (16) can be rewritten to the following form

$$\underline{y} = Ax + \underline{e}. \tag{17}$$

Due to the space constraint, the expression of the design matrix A is omitted here, and the unknown parameters and the measurements in (17) can respectively be described as

$$x = \left[a(t_1) - a^0(t_1) \quad b(t_1) - b^0(t_1) \quad a(t_2) - a^0(t_2) \quad b(t_2) - b^0(t_2) \quad M_{f,1} \quad M_{f,2} \quad M_{f,3} \quad M_{f,4} \right]^T;$$

$$\begin{aligned}\underline{y} = \Big[&\underline{\Phi}^1_{-k,k}(t_1) + 2\pi f_c r_1^0(t_1) \quad \underline{\Phi}^2_{-k,k}(t_1) + 2\pi f_c r_2^0(t_1) \quad \underline{\Phi}^3_{-k,k}(t_1) + 2\pi f_c r_3^0(t_1) \quad \underline{\Phi}^4_{-k,k}(t_1) + 2\pi f_c r_4^0(t_1) \\ &\underline{\Phi}^1_{-k,k}(t_2) + 2\pi f_c r_1^0(t_2) \quad \underline{\Phi}^2_{-k,k}(t_2) + 2\pi f_c r_2^0(t_2) \quad \underline{\Phi}^3_{-k,k}(t_2) + 2\pi f_c r_3^0(t_2) \quad \underline{\Phi}^4_{-k,k}(t_2) + 2\pi f_c r_4^0(t_2) \Big]^T;\end{aligned}$$

in which $a^0(\cdot)$ and $b^0(\cdot)$ denote the initial value (or iteratively updated value) of the unknown coordinates of the receiver, and $r^0(\cdot)$ denotes the initial value of the geometric distance.

The variance of the phase measurement can be derived from the signal model. Due to space constraints, the derivation is omitted here, and the reader is referred to the Appendix. For sufficiently large SNR, the phase measurement from the k-th sub-carrier approximately satisfies the following distribution

$$\underline{\Phi}_k \sim \mathcal{N}(\Phi_k, 1/2\mathrm{SNR}).$$

The carrier phase is derived from the combination of the two symmetrically located pilot sub-carriers, although the SCO is introduced in the signal model, the impact of the SCO η can be ignored (as shown in (11)). Thus, the distribution of the carrier phase measurement can approximately be given without considering the SCO as

$$\underline{\Phi}_{-k,k} \sim \mathcal{N}(\Phi_{-k,k}, 1/4\mathrm{SNR}). \tag{18}$$

Based on the linearized observation model, we can solve equation (17) via the least-squares estimation (LSE) method. If all measurements are independent and identically distributed, the unknown estimators can be obtained from

$$\underline{\hat{x}} = (A^{\mathrm{T}}A)^{-1}A^{\mathrm{T}}\underline{y}. \tag{19}$$

In addition, the variance can be derived from

$$Q_{\hat{x}\hat{x}} = \left(A^{\mathrm{T}}Q_{yy}^{-1}A\right)^{-1},\ Q_{yy} = (1/4\mathrm{SNR})I_8,$$

where I_8 stands for an eight-by-eight identity matrix.

SIMULATION

We consider an OFDM based IEEE802.11p system, which is designed for Vehicle-to-Vehicle (V2V) and Vehicle-to-Infrastructure (V2I) communication, as a potential system for positioning and navigation. Since the sub-carrier spacing in IEEE802.11p signals is relatively large, the ICI due to the Doppler effect is not significant and can be further ignored [13].

The positioning scenario that is used in the simulation is shown in Fig .1, in which there are four transmitters with fixed and known locations, and a rover receiver is moving with a constant velocity. The noise level of received signals from different transmitters is assumed as identical (i.e., same SNR). Some key simulation parameters are shown in Table 1.

Table 1 Simulation parameters of an OFDM-based Positioning system

Simulation parameters	Value	Simulation parameters	Value
Physical layer	OFDM	Num. of subcarriers	64
Total symbols in one frame	100	Cyclic prefix	16 samples
Total OFDM frame	400	Velocity of Rx	80 km/h
Central frequency	5.9 GHz	Signal-to-Noise Ratio	20 dB
Bandwidth	10 MHz	Pilot subcarriers k used for phase measurements	{-12, 12}

First, we only consider the carrier frequency offset due to the Doppler shift; the sampling clocks of the receiver and the transmitters are assumed synchronized (i.e. no SCO). The phase of the pilot sub-carriers can be simply obtained from channel estimation. Since k = {-12,12} sub-carrier are chosen as the pilot sub-carriers, the carrier phase can be derived (14). Fig. 2(a) shows the wrapped carrier phase measurements. For comparison purpose, the physical carrier phase is also shown in this figure as `true value'. The phase rotation of a complex number should be always between -π and π in radian, so the true wrapped carrier phase shown in Fig. 2(a) varies from -180 to 180 degree.

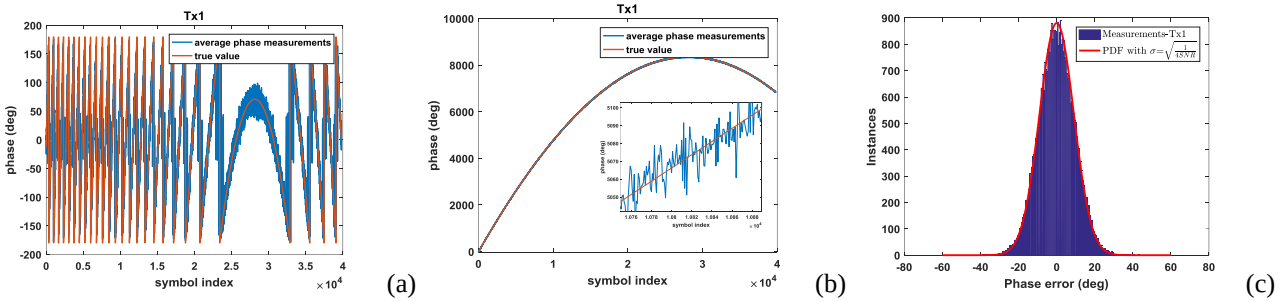

Fig. 2 Plots of single-difference phase measurements and physical true phase value for the Tx1, when the SNR is 20dB, and the symbol length is 8 μs. (a) wrapped phase measurements obtained from channel estimation; (b) unwrapped phase measurements, (c) histogram of the phase error of Tx1 with a SNR of 20 dB, with the PDF of the Gaussian distribution with $\sigma = \sqrt{1/4\mathrm{SNR}}$

In order to keep the phase ambiguity M in (14) as a constant value through the entire observation interval, the phase measurements should be unwrapped, which can be achieved by detecting the phase jumps that are greater than π. The unwrapped carrier phase measurements through 400 OFDM frames are shown in Fig. 2(b). In order to present the difference between the average phase measurements and the physical carrier phase removed the initial phase ambiguity, we simply calculate the difference between these two values (see Fig. 2(c)). The standard derivation of the phase error is 9.297 degree in such a case, which also aligns with the value derived from (18).

The carrier phase measurements of four transmitters are shown in Fig. 3(a). Then, the unknown coordinates of the receiver can be derived from (16). Since the Gauss-Newton method is applied here to solve the non-linear least-squares

estimation problem, the initial values of the unknown coordinates are set to the true value. Thus, the iteration is omitted in this simulation. Though the phase can be measured from every OFDM symbol, it is unnecessary to calculate the coordinates of the receiver for every OFDM symbol, because the receiver moves less than 0.01m along the x-direction within 10 OFDM symbols. Therefore, in (14), the phase measurements at time epoch t_1 is chosen as the first carrier phase measurement, and the measurements at time epoch t_2 are updated each time after 10 OFDM symbols.

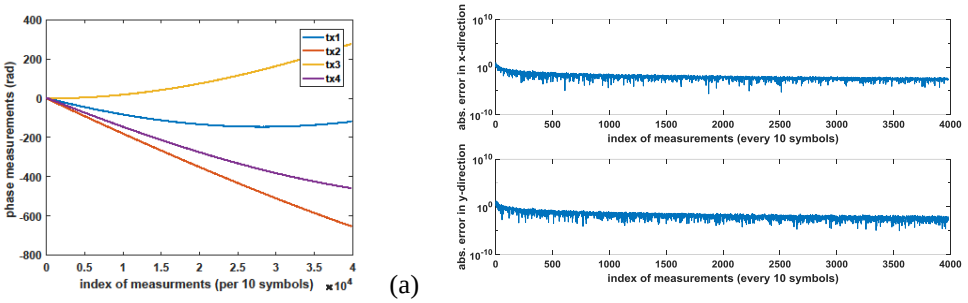

(a) (b)

Fig. 3(a) the unwrapped phase measurements of the transmitter Tx1, Tx2, Tx3 and Tx4, and SNR=20dB. (b) absolute position error in the x-direction (upper) and in the y-direction (lower) and SNR=20dB. Each time only two measurements epochs along the horizontal axis are used.

Furthermore, Fig. 3(b) shows the positioning error along the x-direction and the y-direction, respectively. The positioning error decreases with an increasing time difference. At the beginning, for instance, before the 500-th measurement (representing a time duration of 0.04s), the geometry at t_1 and t_2 is relative similar resulting in a poor design matrix A in (17) nearly rank-defect. Therefore, the root-mean-square error (RMSE) is derived from the measurements after the 500-th measurement which roughly indicates that improvement in precision levels off. Based on the simulation result shown in Fig. 3(b), the RMSE along the x-direction is 0.006m; and the RMSE along the y-direction is 0.024m.

For comparison, positioning based on time-delay estimation (TDE) is also simulated here. This can be seen as pseudo-range code measurements in the GNSS. Based on the super-resolution method ESPRIT, the propagation time delay can be derived from the long training symbol. For more details, readers can refer to the reference [14]. As an example, Fig. 4(a) presents the true propagation time delay and the ESPRIT based time-delay estimation in terms of Tx1. We simulate 400 OFDM frames (approximately 7.5 m of displacement), and the propagation time delay is estimated based on the first OFDM long training symbol in every OFDM frame. The RMSE of TDE is about $0.02\,T_s$ ($T_s = 0.1\mu s$ in this simulation), which can be converted to distance as 1.2m.

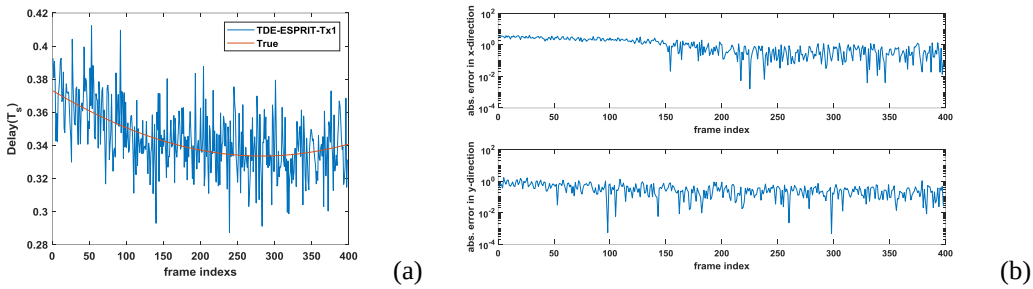

(a) (b)

Fig. 4 (a) ESPRIT based time-delay measurements (with the sampling interval $T_s = 10^{-7}\,s$) for Tx1, and SNR=20dB, (b) the absolute position error along the x-direction and the y-direction, and SNR=20dB, ESPRIT is applied for time-delay measurements and the update rate is one OFDM frame.

By using the same approach, the propagation time delay of the direct path can be measured for all transmitters. After solving a non-linear estimation problem, the absolute position error along the x-direction and y-direction are presented in Fig. 4(b). The RMSE of the x-direction and the y-direction are 1.247m and 0.375m, respectively. Positioning based purely on the carrier phase measurement, though it requires a change of the geometry (i.e., the receiver has to move around), it largely outperforms the positioning based on time delay measurements.

In addition, we can also introduce the sampling clock error η in this OFDM based positioning system, but its major impact can be cancelled in the combination of two symmetrically located pilot sub-carriers. Though there is a residual part that remains in carrier phase measurements, it can be ignored as shown in (11). However, due to the sampling clock offset, a timing synchronization offset Δ may also occur. But this offset can still be eliminated based on the phase combination. On the other hand, due to a timing synchronization error, the time-delay estimation based on the ESPRIT method may include different biases in different OFDM frames. Thus, positioning based on the ESPRIT time delay estimation is not feasible in the presence of the timing synchronization error. With a fixed 50ppm sampling clock error, the RMSEs of positioning based on carrier phase measurements are presented in Table 2.

Table 2 RMSE of positioning error along the x-direction and the y-direction, in which the carrier phase based positioning error is evaluated without a sampling clock offset (0 ppm) and with a fixed sampling clock offset (50 ppm); the ESPRIT time delay measurements based positioning error is only analyzed when there is no sampling clock error in the system.

	SCO: 0 ppm		**SCO: 50 ppm**	
Measurements	RMSE-x(m)	RMSE-y(m)	RMSE-x(m)	RMSE-y(m)
Carrier phase	0.0084	0.0292	0.0095	0.0301
ESPRIT time delay	1.247	0.375	/	/

CONCLUSION

In this paper, OFDM signals have been used as signals of opportunity for positioning. The carrier phase measurements were derived from the average of the phase measurements from two symmetrically located sub-carriers. Moreover, the impact of the sampling clock offset and timing synchronization error can largely be removed by applying the linear phase combination; only the carrier phase change due to the Doppler effect remained in the phase measurements. For a large SNR, the estimation of the sub-carrier phase is unbiased, and it can be approximated as a Gaussian distribution with variance 1/4SNR. With a 50 ppm sampling clock frequency offset, the positioning through carrier phase measurements reached a decimetre level accuracy for 99% of the cases.

Though positioning through pure carrier phase measurements requires the geometry of the positioning scenario to change, in other words, the receiver has to move around and the signal should also be transmitted and received continuously, it can achieve a more accurate positioning result compared to the one based on time delay measurements. Because time delay measurements are mainly derived from the cross-correlation between the received signal and the local generated reference signal or a super-resolution method (e.g., ESPRIT), their accuracies are limited by the signal bandwidth and the subcarrier spacing. Thus, given a continuously transmitted OFDM signal with a relative narrow bandwidth (e.g., 10-20MHz), positioning based on carrier phase measurements is a promising approach to improve its accuracy. However, the carrier phase measurements can easily be perturbed by multipath, thus, further research should be directed to estimate the carrier phase of the LoS component in a multipath condition.

APPENDIX

In this appendix the statistical distribution of the phase measurement is derived.

Considering zero-mean additive complex white Gaussian noise for the received signal as shown in (6), and defined as

$$\begin{bmatrix} \Re\{\underline{w}_n\} \\ \Im\{\underline{w}_n\} \end{bmatrix} \sim \mathcal{N}\left(\begin{bmatrix} 0 \\ 0 \end{bmatrix}, \begin{bmatrix} \sigma_w^2 & 0 \\ 0 & \sigma_w^2 \end{bmatrix} \right), \tag{20}$$

where $\Re$ and $\Im$ denote the real and imaginary part of the complex value, respectively. Consequently, after Fourier transformation the received data on the k-th subcarrier can be given as

$$\underline{R}_k = R_k + \mathcal{F}\{\underline{\mathbf{w}}\} = R_k + \underline{W}_k, \tag{21}$$

where $\underline{\mathbf{w}}$ denotes measurement noise vector.

If the pilot symbols are taken from a BPSK constellation (i.e., $|c_k|=1$), then the noise term in the channel estimation shown in (12) should be statistically equivalent to $\mathcal{F}\{\underline{\mathbf{w}}\}$. With the DFT of the complex white noise as

$$\underline{W}_k = \mathcal{F}\{\underline{\mathbf{w}}\} = \sum_{n=0}^{N-1} \underline{w}_n e^{-j2\pi\frac{kn}{N}} = \underline{U}_k + j\underline{V}_k .$$

The distribution of $\underline{W}_k$ can be derived as follows

$$\begin{bmatrix} \underline{U}_k \\ \underline{V}_k \end{bmatrix} \sim \mathcal{N}\left(\begin{bmatrix} 0 \\ 0 \end{bmatrix}, \begin{bmatrix} N\sigma_w^2, & 0 \\ 0, & N\sigma_w^2 \end{bmatrix} \right).$$

Furthermore, as a means to derive the distribution of phase observables, the complex Gaussian noise $\underline{W}_k$ can be projected onto the signal R_k. The phase measurement $\underline{\Phi}_k$ can be derived with (21) as

$$\underline{\Phi}_k = \arctan\frac{\Im(R_k + \underline{W}_k)}{\Re(R_k + \underline{W}_k)} = \arctan\frac{\Im(R_k)}{\Re(R_k)} - \arctan\frac{P_{R_k}^{\perp}\underline{W}_k}{R_k + P_{R_k}\underline{W}_k}, \tag{22}$$

where $P_{R_k}\underline{W}_k$ and $P_{R_k}^{\perp}\underline{W}_k$ are orthogonal projectors, $P_{R_k}\underline{W}_k$ is produced by projecting $\underline{W}_k$ onto R_k, and $P_{R_k}^{\perp}\underline{W}_k$ is generated by projecting $\underline{W}_k$ along the orthogonal complement of R_k. Moreover, because of the complex Gaussian noise $\underline{W}_k$, $P_{R_k}^{\perp}\underline{W}_k$ and $P_{R_k}\underline{W}_k$ also satisfy the Gaussian distribution. Considering a high SNR condition, we have

$$R_k + P_{R_k}\underline{W}_k \approx R_k ,$$

and equation (22) can be written as

$$\underline{\Phi}_k \approx \arctan\frac{\Im(R_k)}{\Re(R_k)} - \arctan\frac{P_{R_k}^{\perp}\underline{W}_k}{R_k} = \Phi_k - \underline{\varphi}_k .$$

Utilizing the Taylor series expansion for the ' arctan ' of the noise component and assumed a high SNR condition, the signal component R_k will be much larger than the projection of the noise component.

Therefore, the phase measurements under a high SNR condition can also be assumed approximately Gaussian distributed

$$\underline{\Phi}_k \overset{a}{\sim} \mathcal{N}(\Phi_k, \sigma_{\Phi}^2) ,$$

where *a* denotes 'approximate', and the variance can further be derived by applying the error propagation theorem [12]. Since the projected vector can be written as

$$\begin{bmatrix} P_{R_k}\underline{W}_k \\ P_{R_k}^{\perp}\underline{W}_k \end{bmatrix} = \begin{bmatrix} \cos(\Phi_k), & \sin(\Phi_k) \\ -\sin(\Phi_k), & \cos(\Phi_k) \end{bmatrix} \begin{bmatrix} \Re\{\underline{W}_k\} \\ \Im\{\underline{W}_k\} \end{bmatrix}.$$

So that we have

$$\sigma^2_{P_{R_k}^{\perp}\underline{W}_k} = N\sigma_w^2;\ \sigma_{\Phi}^2 = \sigma_{\varphi}^2 = \frac{N\sigma_w^2}{R_k^2} ,$$

where the variance of the phase measurement depends on the FFT size. But without loss of generality, only one pilot subcarrier is used to measure the arrival phase in the following derivation. According to Parseval's theorem

$$\sum_{n=0}^{N-1}|r[n]|^2 = \frac{1}{N}\sum_{k=-N/2+1}^{N/2}|R_k|^2 , \tag{23}$$

also due to the identical modulation for all the pilot sub-carriers (i.e. BPSK), thus the power is uniformly distributed among them. Due to the independent and identically distributed AWGN shown in (20) among different samples, the power of the received complex noise from *N* samples is $2N\sigma_w^2$. Thus the distribution of the phase measurement that depends on SNR can be written with (23) as

$$\mathrm{SNR} = \frac{\frac{1}{N}NR_k^2}{2N\sigma_w^2} = \frac{R_k^2}{2N\sigma_w^2} , \quad \underline{\Phi}_k \overset{a}{\sim} \mathcal{N}(\Phi_k, \frac{1}{2\mathrm{SNR}}) .$$

REFERENCES

[1] J. Hightower, R. Want and B. Gaetano, "SpotON: An indoor 3D location sensing technology based on RF signal strength.," 2000.

[2] L. M. Ni, Y. Liu, Y. Lau and A. P. Patil, "LANDMARC: indoor location sensing using active RFID," Wireless Network, vol. 10, no. 6, pp. 701-710, 2004.

[3] Q. Zhang, C. H. Foh, . B.-C. Seet and A. C. M. Fong, "RSS ranging based Wi-Fi localization for unknown path loss exponent," in Global Telecommunications Conference (GLOBECOM 2011), 2011 IEEE, 2011.

[4] A. Makki, A. Siddig, M. M. Saad, C. Bleakley and J. Cavallaro, "High-resolution time of arrival estimation for OFDM-based transceivers," Electronics Letters, vol. 51, no. 3, pp. 294-296, 2015.

[5] A. Makki, A. Siddig, M. M. Saad, J. R. Cavallaro and C. J. Bleakley, "Indoor Localization Using 802.11 Time Differences of Arrival," IEEE Trans. Instrumentation and Measurement, vol. 65, no. 3, pp. 614-623, 2016.

[6] F. Zhao, W. Yao, C. C. Logothetis and Y. Song, "Comparison of super-resolution algorithms for TOA estimation in indoor IEEE 802.11 wireless LANs," in International Conference on Wireless Communications, Networking and Mobile Computing, 2006.

[7] K. Pahlavan, X. Li and J.-P. Makela, "Indoor geolocation science and technology," IEEE Communications Magazine, vol. 40, no. 2, pp. 112-118, 2002.

[8] D. Vasisht, S. Kumar and D. Katabi, "Decimeter-Level Localization with a Single WiFi Access Point," in NSDI, 2016.

[9] P. Teunissen and O. Montenbruck, Springer Handbook of Global Navigation Satellite Systems, Springer, 2017.

[10] C. Yang, L. Chen, O. Julien, A. Soloviev and R. Chen, "Carrier Phase Tracking of OFDM-Based DVB-T Signals for Precision Ranging," in ION GNSS+ 2017, 30th International Technical Meeting of The Satellite Division of the Institute of Navigation, 2017.

[11] Y. G. Li and G. L. Stüber, Orthogonal frequency division multiplexing for wireless communications, springer Science & Business Media, 2006.

[12] H. Jiang, S. Cai, W. Xiang and H. Qian, "Dynamic Channel Estimation over Fast Time-varying Channel for Vehicle Wireless Communications," in International Wireless Internet Conference, 2013.

[13] P. Teunissen, D. Simons and C. Tiberius, Probability and Observation Theory., Technische Universiteit Delft, 2004.

[14] B. Yang, K. B. Letaief, R. S. Cheng and Z. Cao, "Channel estimation for OFDM transmission in multipath fading channels based on parametric channel modeling," IEEE transactions on communications, vol. 49, no. 3, pp. 467-479, 2001.